nature portfolio

https://doi.org/10.1038/s41561-021-00727-y

Supplementary information

Long-lived shallow slow-slip events on the Sunda megathrust

In the format provided by the authors and unedited

Supplement for "Long-lived shallow slow-slip events on the Sunda megathrust"

Rishav Mallick[1,2], Aron J. Meltzner[1,2], Louisa L.H. Tsang[3,4], Eric O. Lindsey[2,5], Lujia Feng[2], and Emma M. Hill[1,2]

[1]Asian School of the Environment, Nanyang Technological University, Singapore
[2]Earth Observatory of Singapore, Nanyang Technological University, Singapore
[3]Universite Cote d'Azur, CNRS, Observatoire de la Cote d'Azur, IRD, Geoazur, Campus CNRS, Sophia Antipolis, Valbonne, France
[4]University of Surrey, International Study Centre, Guildford, United Kingdom
[5]Department of Earth and Planetary Sciences, University of New Mexico, Albuquerque, New Mexico, United States of America

Description of Contents

This document contains 2 text sections and 3 figures.
In Text S1, we discuss the mechanism of generating Slow Slip Events (frictional instabilities) on velocity-weakening and velocity-strengthening faults whose fault strength evolution is given by rate-state friction.
In Text S2, we discuss the Enggano section of the Sunda megathrust; we first describe the GPS and seismological observations from this island, and then explore different earthquake cycle models that can explain the observed deformation pattern there.

Figures

- S1 - SSE generated by velocity-strengthening versus velocity-weakening frictional instabilities
- S2 - Slip rate evolution for an SSE generated on a velocity-strengthening fault
- S3 - GPS deformation observations and model for Enggano

S1. Slow Slip Events (SSE) on faults governed by rate-state friction

Governing Equations

We can describe the variation of the friction coefficient on a thrust fault as a function of fault velocity v, and a state parameter θ which represents the average duration of asperities, using rate-and-state dependent friction and the ageing law (Dieterich 1979; Ruina 1983).

$$\mu = \mu_0 + a \log\left(\frac{v}{v_0}\right) + b \log\left(\frac{v_0 \theta}{L}\right) \tag{S.1}$$

$$\frac{d\theta}{dt} = 1 - \frac{v\theta}{L} \tag{S.2}$$

μ_0, v_0 are reference values of the friction coefficient and velocity respectively; a, b are material properties that describe the evolution of the friction coefficient to changes in velocity and its evolution in time (and slip, by extension) respectively, while L is the critical slip distance over a population of frictional contacts evolve.

Consider the force balance on the fault, we equate the stresses arising from elastic interaction with friction and radiation damping as follows:

$$\dot{\tau}^{\infty} t + K\delta = \mu\bar{\sigma} + \frac{G}{2v_s} v \tag{S.3}$$

Here $\dot{\tau}^{\infty}$is the far field stressing rate on the fault (derived from loading the fault at a slip rate of V_{pl}), K is the elastic interaction kernel computed from the analytical solutions for stress due to a shear crack in an elastic medium (plane strain) (Segall 2010). The right hand side contains the frictional stress ($\bar{\sigma}$ is the normal stress) and the last term is the radiation damping approximation (Rice1986,Rice1993) (G is the shear modulus and v_s is the shear wave speed in the medium).

The time derivative of the force balance (Equation S.3) gives us the momentum balance. For simplification we use the following variable transformations:

$$\begin{aligned} \zeta &= \log \frac{v}{v_0} \\ \phi &= \log \frac{v_0 \theta}{L} \end{aligned} \tag{S.4}$$

Using these transformations in the time derivative of Equation S.3 with Equation S.1 and S.2, we obtain the governing equation (momentum balance) to generate earthquake sequences:

$$\begin{gathered} \dot{\tau}^{\infty} + K v_0 \exp\zeta = \left(a\dot{\zeta} + b\dot{\phi}\right)\bar{\sigma} + \frac{G}{2v_s}\left(v_0 \exp\zeta\right)\dot{\zeta} + \left(\mu_0 + a\zeta + b\phi\right)\dot{\bar{\sigma}} \\ \dot{\bar{\sigma}} \to 0 \text{ or kinematically imposed} \end{gathered} \tag{S.5}$$

We solve for unknown variables $\zeta, \phi, \bar{\sigma}$ by numerically integrating the above coupled ODEs (Equation S.5 and S.2) using a 4th order Runge-Kutta adaptive time-stepping method, subject to an arbitrary initial condition $\left(\zeta^0 = 10^{-3}, \phi^0 = 0, \bar{\sigma}^0 = 60MPa\right)$.

SSE on velocity-weakening faults
To generate SSE on velocity-weakening (VW implies the friction coefficient decreases with an increase in velocity, thereby localizing strain and promoting unstable fault slip) faults, we use an instability nucleation size comparable to the dimension of the the VW region (R). We assume the earthquake cycle is driven only by shear tractions and thus neglect any temporal variation in the fault normal stress ($\dot{\bar{\sigma}} = 0$).

Simple stability analysis of this system of equations gives us a nucleation size (James R. Rice 1993) for a VW frictional instability as:

$$h^* = \frac{GL}{(b-a)\bar{\sigma}} \tag{S.6}$$

For $\frac{R}{h^*} \sim 1.1$, we generate frictional instabilities which correspond to SSE (Figure S1A) where with increasing slip, the rate of elastic energy release exceeds the frictional weakening thereby preventing the instability from running away to seismic slip rates.

A characteristic feature of these kinds of SSE are that they have a long nucleation phase, where fault slip rate accelerates over a time interval comparable to the interval over which the SSE shows almost linear displacement timeseries (Figure S1B). This means that for an SSE to have an average slip rate of 1-1.5 V_{pl} over a period of 10-20 years, it must be preceded by an acceleration on the fault lasting 10-20 years. However this is not observed in coral timeseries, and so is an unsatisfactory explanation.

Instead, we observe an abrupt velocity change and so the underlying mechanism needs to produce a sudden change in velocity (at a timescale significantly shorter than the SSE duration itself) while still creeping at a rate comparable to the plate loading rate.

SSE on velocity-strengthening faults
Frictional instabilities do not typically nucleate on velocity-strengthening (VS) faults because an increase in fault strength with increase in fault slip rates implies that instabilities are damped out. However, unstable frictional behaviour on VS faults can occur due to two reasons: (1) A decrease in the effective normal stress on the fault, due to evolution of fluid pressures, weakens the fault and counters the velocity damping the VS material would have otherwise executed. (2) When a VS fault is perturbed away from its steady-state creep behaviour, by a past negative stress drop event, the evolution of the state-parameter (θ) can promote mildly unstable frictional behaviour.

We exploit both mechanisms and propose a hybrid mechanism where the nucleation of an instability initiates as the fault recovers from a previous negative stress drop event; this velocity increase is coupled with gouge compaction and the release of pore fluids onto the fault (Perfettini and Ampuero 2008), which further weaken the frictional strength and cause the instability to last up to 3 decades.

We solve the governing equations for velocity, state and normal stress evolution detailed in Equations S.2, S.5 subject to an initial condition. We model the initial condition with an instantaneous pore-fluid expulsion event ($t^- \to t^+$), possibly caused by a previous great earthquake, which drained the fault and dropped $\bar{\sigma}$ by ~ 2 MPa (Figure 3, S1C).
This condition is obtained by computing an effective change in ζ, ϕ from Equation S.3 for an instantaneous change in normal stress from $\bar{\sigma}^- \to \bar{\sigma}^+$.

$$\mu_0 \left(\bar{\sigma}^+ - \bar{\sigma}^-\right) + a\left(\bar{\sigma}^+\zeta^+ - \bar{\sigma}^-\zeta^-\right) + b\left(\bar{\sigma}^+\phi^+ - \bar{\sigma}^-\phi^-\right) = 0 \tag{S.7}$$

Since this is an instantaneous event, we assume the change in elastic interactions is negligible in Equation S.3 implying the only change in the force balance is in the frictional strength (Equation S.7).

The instantaneous event also implies that the state variable has not evolved from $t^- \to t^+$ i.e. $\phi^- = \phi^+$. Simplifying this, we can write:

$$(\mu_0 + b\phi)\left(\bar{\sigma}^+ - \bar{\sigma}^-\right) + a\left(\bar{\sigma}^+\zeta^+ - \bar{\sigma}^-\zeta^-\right) = 0 \tag{S.8}$$

We provide an expression for ζ^+ which serves as the initial condition for the momentum balance.

$$\zeta^+ = \frac{\sigma^-}{\sigma^+}\zeta^- - \left(\frac{\mu_0 + b\phi}{a}\right)\left(1 - \frac{\sigma^-}{\sigma^+}\right) \tag{S.9}$$

We impose Equation S.9 on Equation S.5 at $t = 50yrs$ (Figure S1C) and numerically integrate it using a Runge-Kutta 4^{th} order finite difference method which allows adaptive time stepping.
The instability initiates spontaneously around 200 yrs as the velocity on the fault tries to reach its steady state value (Figure S1D, S2). In the absence of any additional weakening such an instability arrests itself and is limited to a slip rate indistinguishable from steady-state fault creep (Figure S2). We add slip rate driven pore-pressure rise as an additional source of weakening to reproduce the multi-decadal nature of the SSE (Figure S1).

Pore-pressure evolution
Our exploration of pore-pressure driven fault weakening is motivated by the *fault-valve* model (Sibson 1990). The basic premise is that frictional sliding is a self-sealing process where slow fault shear promotes the formation of a low-permeability fluid barrier through precipitation/dissolution of insoluble/soluble phases or pressure solution creep that closes pore space (porosity) in the gouge (Gratier et al. 2002), thereby building overpressure and decreasing fault strength. At the earthquake cycle timescale, it is thought that on-fault fluid pressure is relieved during earthquakes due to cracking and fracturing of the fault gouge during fast slip; slow interseismic processes are thought to promote compaction and build pore-pressure (Marone, Raleigh, and Scholz 1990; Sibson 1990).

Motivated by laboratory observations and such a conceptual model, typical velocity dependant porosity evolution models are derived to have a logarithmic functional form (porosity $\propto \log(v)$). This porosity evolution equation is then used in a fluid mass balance as an unsteady-state (membrane) diffusion problem to solve for the evolution of pore-fluid pressure (Segall and James R Rice 1995). This formulation creates a strong dependence of pore-pressure on velocity and the state variable (v, θ), but erases any influence of cumulative slip (or shear). However, experimental investigations of the variation of gouge porosity with shear is observed to be more complex, as gouges follow an initial shear-driven compaction phase which is then replaced by a shear rate-dependance (Marone, Raleigh, and Scholz 1990). Additionally the porosity evolution equations are calibrated for sliding experiments run at $\sim 10^{-6}$m/s (Marone, Raleigh, and Scholz 1990), which is orders of magnitude faster than the rates at which we observe the long-lived SSE at Simeulue.

With these considerations in mind, and being mindful of the fact that we know very little about the lithology and the strain history of the Sunda megathrust at the location where we infer the shallow SSE, as well as the exact form of pore-pressure evolution at very low slip rates, we chose to model the rate of pore-fluid pressure rise during the spontaneously-nucleated SSE period as a linear function in time with the normal stress at the end of the SSE restored to its pre-perturbation value (60 MPa in this case). This is conceptually similar to the numerical model of Sleep and Blanpied 1992, where they allowed porosity reduction due to gouge compaction during interseismic creep to drive earthquake cycles.

$$\begin{aligned} \dot{\bar{\sigma}} &= 0 && t \in \left[t^+, t_{SSE}\right] \\ \dot{\bar{\sigma}} &= \frac{2\left(\bar{\sigma}^+ - \bar{\sigma}^-\right)}{\Delta t_{SSE}}\left(1 - \frac{t - t_{SSE}}{\Delta t_{SSE}}\right) && t \in \left[t_{SSE}, t_{SSE} + \Delta t_{SSE}\right] \end{aligned} \tag{S.10}$$

An SSE produced by this mechanism displays piece-wise linear displacement timeseries (Figure S1D), and is preceded by an undetectable fault acceleration (Figure S2), since this occurs at values below the detectable threshold of surface data. Therefore, we consider this as a likely mechanism for shallow long-lived SSE since it can reproduce all the salient features of the coral timeseries and agrees with the frictional properties inferred for this segment of the Sunda megathrust (abrupt velocity change, the magnitude of the velocity change is comparable to the plate velocity, the SSE lasts for 3 decades, and it occurs on the same part of the fault that showed significant afterslip following the 2005 M_w 8.6 Nias earthquake (Qiu et al. 2019).

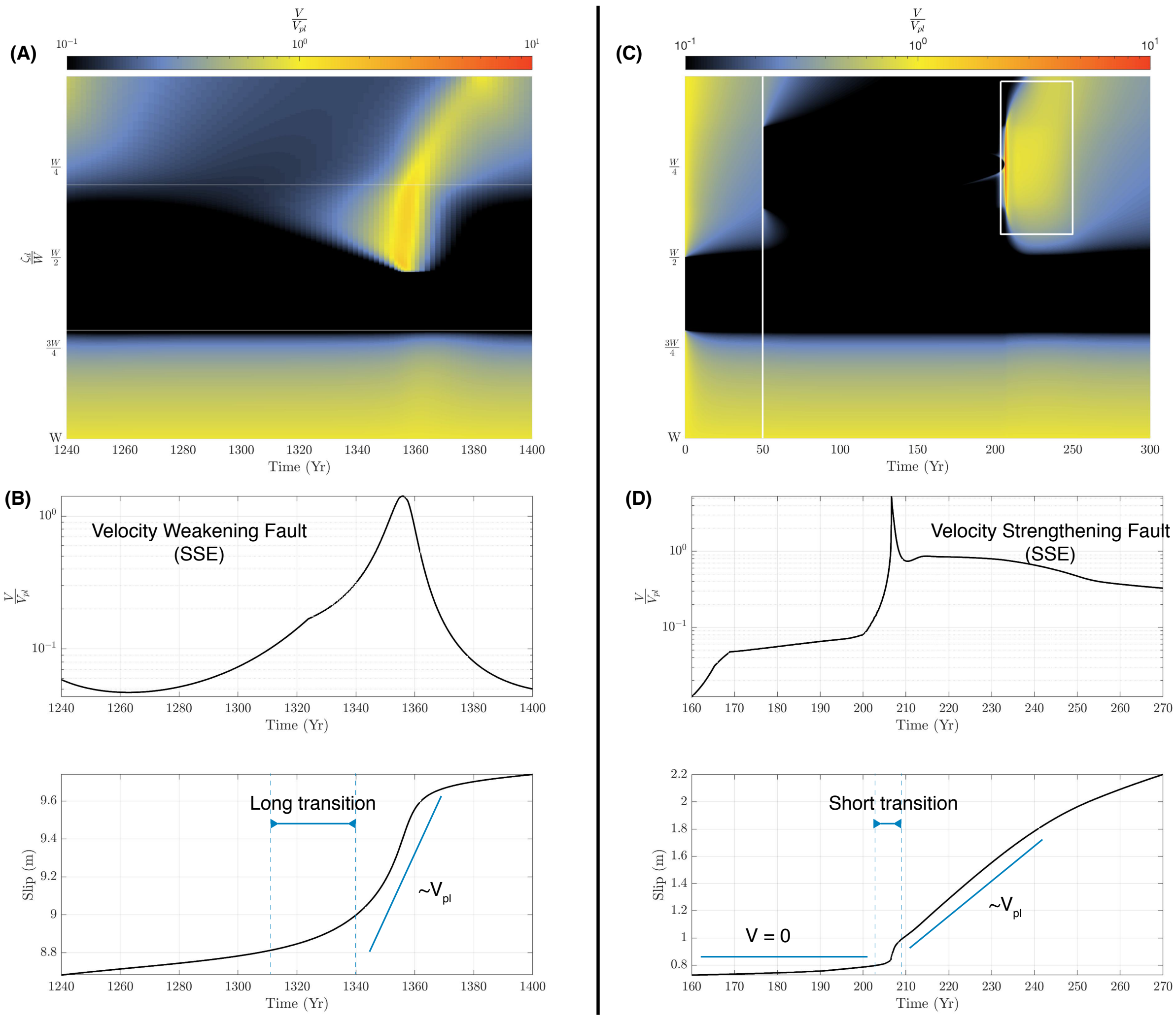

Figure S1: Comparison between SSE on velocity-weakening (VW) and velocity-strengthening (VS) faults. (A) and (C) show the slip rate evolution during the pre-SSE and SSE periods for the VW and VS case respectively. (B) and (D) show the mean slip rate and cumulative fault slip for both cases. The VS fault shows a short transition time between being stationary to creeping at the plate rate or faster; this key feature matches the coral data.

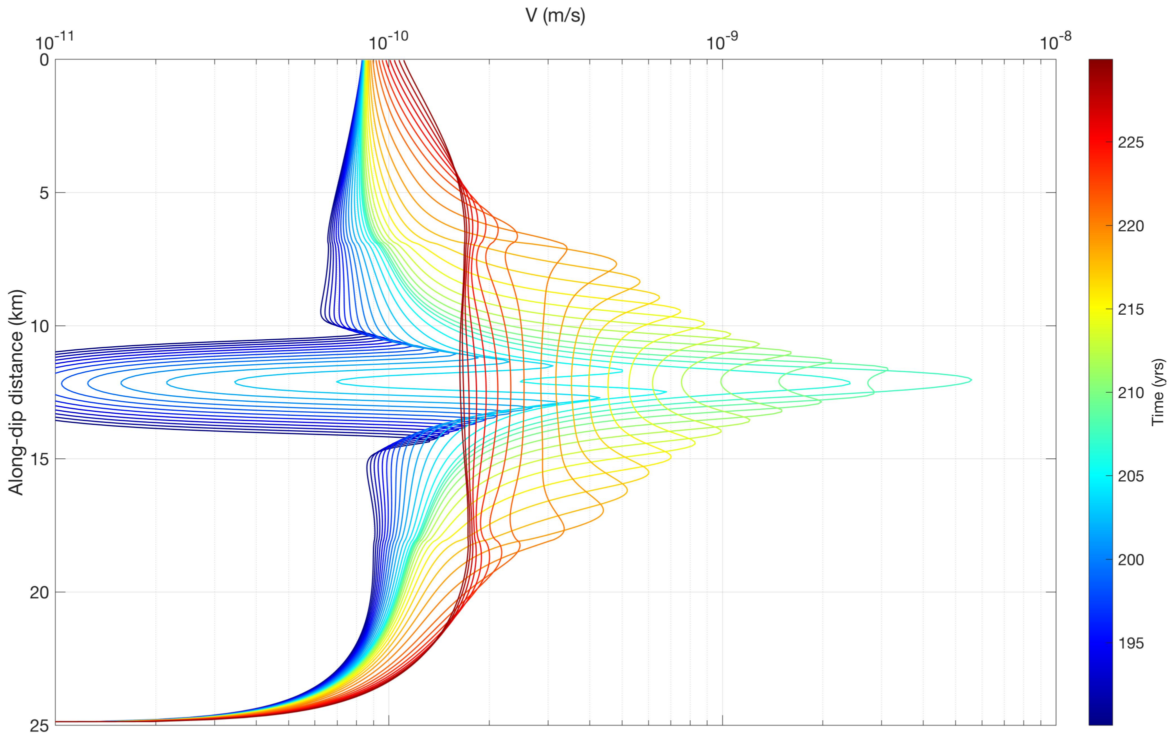

Figure S2: Snapshots through time of a frictional instability on a velocity strengthening fault. A steady-state creeping fault was perturbed early in the simulation (t = 50 yrs) by a pore-fluid expulsion event and allowed to evolve. In this simulation we do not allow additional weakening from pore-pressure recovery on the fault. The colours represent different time periods (t = 190 to 230 yrs) ranging from the initial acceleration of the SSE (blue) until the instability is arrested and the fault resumes creeping at its steady rate velocity (red). The SSE nucleates at the 12-14 km on the simulated fault, as the fault is trying to recover to its steady state creep rate. However, an overshoot of slip rates occurs leading to a pulse of high slip rate at the center of the simulated fault. The transition from creep at below $10^{-10} m/s$ to the accelerated slip pulse of $\sim 10^{-8} m/s$ occurs in a short period of time (1-2 yrs). This instability is then damped out and is smeared over the available fault area over 10-15 years.

S2. Hazard at Enggano

The Enggano segment of the Sunda megathrust behaves markedly differently from the other Sunda megathrust segments such as the Mentawai or Nias-Simeulue segments. There are no documented great earthquakes which have occurred here (Meltzner et al. 2015; Philibosian, Sieh, J.-P. Avouac, et al. 2017; Philibosian, Sieh, J.-p. Avouac, et al. 2014), and the background seismicity indicates a continuously seismically productive megathrust (Figure S3), in contrast to the neighboring segments which showed a marked quiescence before the start of the great earthquakes (M_w9.2 2004 Aceh-Andaman, M_w8.6 2005 Nias-Simeulue and M_w8.4 2007 Bengkulu). The GPS-derived velocity for the Enggano island site (MLKN in Figure S3) is from campaign occupations from 1992-2001 (site name ENGG) (Prawirodirdjo et al. 2010) and a continuous site operated from 2005-onwards (Figure S3A,B). The horizontal velocities from both time periods are significantly different raising the question: why did the velocities change?

We hypothesize that the change is related to an ongoing long-lived shallow SSE (Figure S3A-C). The large landward signal in the campaign GPS velocity indicates that the megathrust under Enggano was frictionally locked (at least within the seismogenic zone) until 2001 (Figure S3C). The horizontal velocity field from 2005-present shows almost exclusively trench-parallel sliver motion, which taken in isolation could imply no frictional locking on the megathrust. However, once we factor in the vertical displacements from MLKN (Figure S3B) we understand that it is not possible for steady aseismic subduction to produce ~ 10 mm/yr of subsidence from 2005-2016. We believe that a shallow ongoing SSE must be the cause of negligible trench-normal motion while compounding the subsidence signal from this island (Figure S3C).

An alternate explanation could be visco-elastic effects of upper mantle deformation due to the $M_w 7.9, 2000$ Enggano intra-slab earthquake. The mantle wedge of the overriding plate, and the mantle of the oceanic plate are thought to deform through viscous processes following stress perturbations from nearby great earthquakes. However, these effects are distributed over a large volume and typically decay exponentially with time since the initial perturbation (for Enggano the last significant stress perturbation was in 2000). Seismicity patterns in a volume near Enggano show no clear deformation trends in space or time (Figure S3D,E) indicating that apart from the time period close to the $M_w 7.9, 2000$ event, the seismic productivity was representative of background processes. It appears that the deformation rates before and after the year 2000 are not distinguishable (for events above M_w4.5 - Figure S3E), thereby negating any justification for visco-elastic relaxation of the mantle driving the observed signal in Figure S3B.

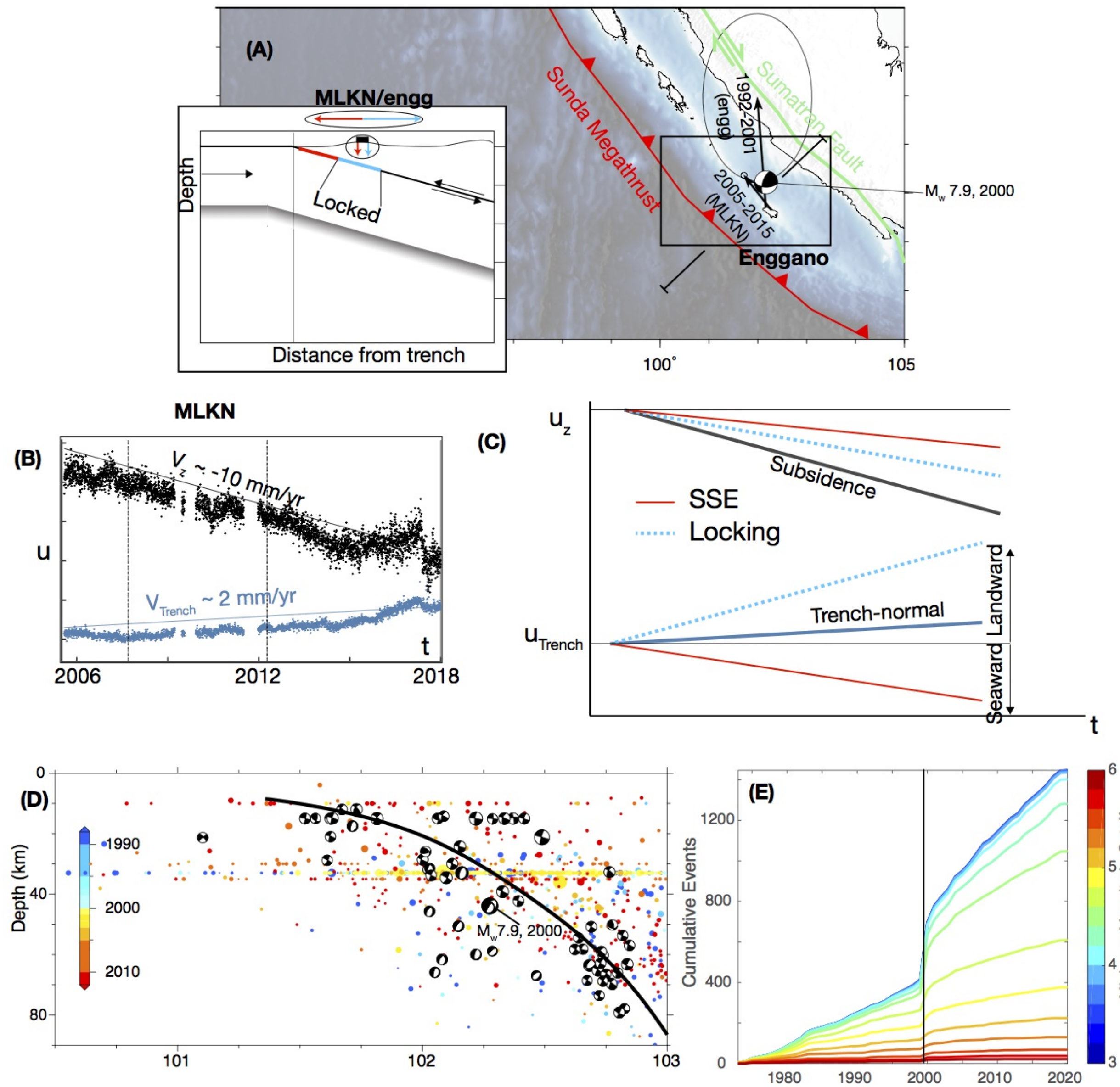

Figure S3: Geodetic and seismotectonic observations near Enggano. (A) We show the horizontal site velocities from a campaign (1992-2001) and continuous (2005-2015) site (MLKN). In the inset we show a schematic cross section of a locked seismogenic zone (cyan) and a shallow SSE region (red) which cause the trench-normal velocity for MLKN to be cancelled out while compounding the subsidence signal. (B) The displacement timeseries (blue - trench-normal motion; black- vertical motion) for MLKN. (C) Schematic to show how the timeseries from the locked (dashed cyan) and SSE region (red) interact together to produce the observations at MLKN. (D) Seismicity from the box shown in (A) plotted in cross section. Circles (coloured by the year) are from the Advanced National Seismic System (ANSS (https://doi.org/10.5066/F7MS3QZH) catalog while beach balls are from Global Centroid Moment Tensor (GCMT Ekström, Nettles, and Dziewoński 2012). The plate boundary (thick black line) is taken from Slab 2 (Hayes et al. 2018). (E) We bin the events based on year and plot them as a cumulative count with time. The different coloured lines indicate a different minimum cutoff for earthquake magnitudes. We vary the minimum cutoff to see if there is a bias in number of reported events because of improvements in methods and/or number of stations.

References

Dieterich, James H. (1979). “Modeling of Rock Friction Experimental 1. Results and Constitutive Equations”. In: *Journal of Geophysical Research* 84.9, pp. 2161–2168. URL: http://dx.doi.org/10.1007/BF00876539%7B%5C%%7D5Cnhttp://www.agu.org/pubs/crossref/1979/JB084iB05p02161.shtml.

Ekström, G., M. Nettles, and A. M. Dziewoński (2012). “The global CMT project 2004-2010: Centroid-moment tensors for 13,017 earthquakes”. In: *Physics of the Earth and Planetary Interiors*. ISSN: 00319201. DOI: 10.1016/j.pepi.2012.04.002.

Gratier, Jean Pierre et al. (2002). “Fluid pressure evolution during the earthquake cycle controlled by fluid flow and pressure solution crack sealing”. In: *Earth, Planets and Space* 54.11, pp. 1139–1146. ISSN: 18805981. DOI: 10.1186/BF03353315.

Hayes, Gavin P. et al. (2018). “Slab2 - A Comprehensive Subduction Zone Geometry Model”. In: *Science* In review.August, pp. 1–10.

Marone, C., C. B. Raleigh, and C. H. Scholz (1990). “Frictional behavior and constitutive modeling of simulated fault gouge”. In: *Journal of Geophysical Research* 95.B5, pp. 7007–7025. ISSN: 01480227. DOI: 10.1029/JB095iB05p07007.

Meltzner, Aron J. et al. (2015). “Time-varying interseismic strain rates and similar seismic ruptures on the Nias-Simeulue patch of the Sunda megathrust”. In: *Quaternary Science Reviews* 122, pp. 258–281. ISSN: 02773791. DOI: 10.1016/j.quascirev.2015.06.003. URL: http://dx.doi.org/10.1016/j.quascirev.2015.06.003.

Perfettini, Hugo and Jean Paul Ampuero (2008). “Dynamics of a velocity strengthening fault region: Implications for slow earthquakes and postseismic slip”. In: *Journal of Geophysical Research: Solid Earth* 113.9, pp. 1–22. ISSN: 21699356. DOI: 10.1029/2007JB005398.

Philibosian, Belle, Kerry Sieh, Jean-Philippe Avouac, et al. (Jan. 2017). “Earthquake supercycles on the Mentawai segment of the Sunda megathrust in the seventeenth century and earlier”. In: *Journal of Geophysical Research: Solid Earth* 122.1, pp. 642–676. ISSN: 21699313. DOI: 10.1002/2016JB013560. URL: http://doi.wiley.com/10.1002/2016JB013560.

Philibosian, Belle, Kerry Sieh, Jean-philippe Avouac, et al. (Sept. 2014). “Rupture and variable coupling behavior of the Mentawai segment of the Sunda megathrust during the supercycle culmination of 1797 to 1833”. In: *Journal of Geophysical Research: Solid Earth* 119.9, pp. 7258–7287. ISSN: 21699313. DOI: 10.1002/2014JB011200. URL: http://doi.wiley.com/10.1002/2014JB011200.

Prawirodirdjo, Linette et al. (Mar. 2010). “Geodetic observations of an earthquake cycle at the Sumatra subduction zone: Role of interseismic strain segmentation”. In: *Journal of Geophysical Research* 115.B3, B03414. ISSN: 0148-0227. DOI: 10.1029/2008JB006139. URL: http://doi.wiley.com/10.1029/2008JB006139.

Qiu, Qiang et al. (July 2019). “Coseismic and Postseismic Slip of the 2005 M w 8.6 Nias-Simeulue Earthquake: Spatial Overlap and Localized Viscoelastic Flow”. In: *Journal of Geophysical Research: Solid Earth* 124.7, pp. 7445–7460. ISSN: 2169-9313. DOI: 10.1029/2018JB017263. URL: https://onlinelibrary.wiley.com/doi/abs/10.1029/2018JB017263.

Rice, James R. (1993). “Spatio-temporal complexity of slip on a fault”. In: *Journal of Geophysical Research* 98.B6, p. 9885. ISSN: 0148-0227. DOI: 10.1029/93JB00191. URL: http://doi.wiley.com/10.1029/93JB00191.

Ruina, Andy (1983). “Slip instability and state variable friction laws”. In: *Journal of Geophysical Research: Solid Earth* 88.B12, pp. 10359–10370. ISSN: 01480227. DOI: 10.1029/JB088iB12p10359. URL: http://doi.wiley.com/10.1029/JB088iB12p10359.

Segall, Paul (Jan. 2010). *Earthquake and Volcano Deformation*. Princeton: Princeton University Press, p. 517. ISBN: 9781400833856. DOI: 10.1515/9781400833856. URL: http://doi.wiley.com/10.1002/0471743984.vse7429%20https://www.degruyter.com/view/books/9781400833856/9781400833856/9781400833856.xml.

Segall, Paul and James R Rice (Nov. 1995). “Dilatancy, compaction, and slip instability of a fluid-infiltrated fault”. In: *Journal of Geophysical Research: Solid Earth* 100.B11, pp. 22155–22171. ISSN: 01480227. DOI: 10.1029/95JB02403. URL: http://doi.wiley.com/10.1029/95JB02403.

Sibson, Richard. H (1990). “Conditions for fault-valve behaviour”. In: 54, pp. 15–28.
Sleep, Norman H. and Michael L. Blanpied (1992). “Creep, compaction and the weak rheology of major faults”. In: *Nature* 359.6397, pp. 687–692. ISSN: 00280836. DOI: 10.1038/359687a0.